Mem. S.A.It. Vol. 89, 274

Memorie della

GPU-accelerated broadband analysis of multi-messenger light curves of GRBs

Maurice H. P. M. van Putten

Physics and Astronomy, Sejong University, 143-747 Seoul, e-mail: mvp@sejong.ac.kr

Abstract. High-frequency multi-messenger observations provide a powerful probe of gamma-ray bursts (GRBs), pioneered by *BeppoSAX* in gamma-rays and LIGO-Virgo in gravitational waves. Identifying the central engines - magnetars or black holes - also promises to improve on GRBs as probes of cosmological evolution. THESEUS' design is ideally suited to pursue both science objectives. Here, we present a general-purpose *graphics processor units* (GPU)-accelerated broadband search algorithm for long duration ascending and descending chirps, post-merger or from core-collapse of massive stars, in electromagnetic and gravitational radiation. It implements butterfly filtering using banks of up to 8 million templates of 1 second duration at over one million correlations per second by heterogeneous computing using a dozen high-end GPUs. We demonstrate its application with the identification of broadband Kolmogorov spectra in long GRBs and the long duration ascending chirp in the merger GW170817. The first shows a noticeable absence of a high frequency bump, otherwise expected from newly formed magnetar central engines. The second illustrates the need for deep searches to identify GRB central engines in descending chirps in gravitational waves, post-merger or from nearby energetic core-collapse supernovae. A future catalogue of THESEUS' GRBs covering a broad range of redshifts may probe the nature of the cosmological vacuum and establish the de Sitter limit as a turning point in cosmological evolution.

Key words. Gamma-ray bursts: observations – black holes: radiation data-analysis: high performance computing – Cosmology: observations

1. Introduction

The nature of the central engine of gamma-ray bursts (GRBs) remains a key outstanding question, currently probed indirectly by multi-wavelength observations in electromagnetic radiation (Piran 2004; Nakar 2007; Zhang et al. 2016; Zigao et al. 2017). Based on total energetics and short-time scale variability (e.g. Sari & Piran 1997; Sari et al. 1998), their central engines are probably magnetars (e.g. Metzger et al. 2011) or black holes (Woosley 1993; Eichler & Levinson 2000; Woosley & Bloom 2006; Woosley 2010). Since short GRBs (SGRBs) and SGRBs with Extended Emission (SGRBEEs) discovered by *Swift* derive from mergers, of neutron stars with another neutron star or black hole, their final remnants should be black holes. While the central engine to the initial short hard spike in SGRBs is uncertain, any Extended Emission *post-merger* lasting tens of seconds is likely associated with a black hole. Detailed spectral-energy relations for Extended Emission (SGREE) and the prompt emission of long GRBs (LGRBs) further show a remarkably common Amati rela-

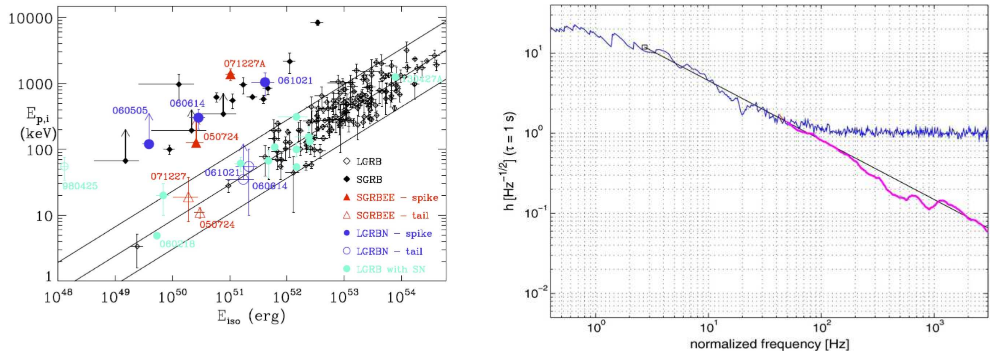

Fig. 1. (Left panel.) The $E_{p,i} - E_{iso}$ plane showing short GRBs with Extended Emission (SGRBEE) and long GRBs with no apparent association with supernovae (LGRBN)(Amati et al. 2002; Amati & Della Valle 2016). Included are GRB-SNe 030329, 050525A, 081007,091127,100316D,101219B along the Amati-relation for normal long GRBs ($\pm 2\sigma$). The sub-energetic GRB980425/SN1998bw is anomalous. The tails of GRBEEs 050724 and 060614 (also a LGRBN) (open triangles, red) falls well within the group of tails of normal LGRB (medium sized filled circles, green). The initial short-hard spike of SGRBEEs (solid triangles, red) falls into the separate group of SGRBs, in common with the initial pulse of LGRBNs (large size filled circle, blue). (Reprinted from (van Putten et al. 2014b).) (Right panel.) The broadband Kolmogorov spectrum (averaged over 42 spectra of long GRBs from *BeppoSAX*) extracted by butterfly filtering using a bank of 8.64 million templates show a featureless extension to over 2 kHz (comoving frame, purple). Noticeably absent is a bump at high frequency, that would otherwise be expected from magnetars newly formed with random orientations of magnetic moment and angular momentum. (Reprinted from (van Putten et al. 2014a).)

tion (Amati et al. 2002) (Fig. 1). Conceivably, therefore, Extended Emission to SGRBs, if present, and long GRBs share a common inner engine: rotating black holes producing extended emission in possibly both the electromagnetic and gravitational-wave spectrum over their lifetime of rapid spin (van Putten & Levinson 2003; van Putten 2012a).

To rigorously identify the central engine to GRBs by gravitational-wave detection (Cutler & Thorne 2002), we propose a focus on high-frequency broadband analysis of contemporaneous emission in electromagnetic and gravitational radiation. While both magnetars and black holes - interacting with high density matter formed post mergers and core-collapse of massive stars - can produce extended emission in the process of spin down, their spectral properties should be quite different. In the electromagnetic spectrum, magnetars newly formed are expected to produce a broadband bump around 2 kHz (co-moving frequency) by generic mis-alignment of magnetic moment and angular momentum, whereas this would be absent for any high-energy emission from black hole outflows by inherent alignment of the same by Carter's theorem (Carter 1968). No such bump is seen in a broadband analysis of light curves of a sample of bright long GRBs from the *BeppoSAX* catalogue (Fig. 1).

Furthermore, any gravitational wave emission from a magnetar or a black hole formed in above mentioned extreme transient events should be a *descending chirp*, as angular momentum carried off in gravitational radiation of a single object causes spin down, as opposed to spin up for binary systems. For magnetars, such descending chirps formally can reach zero frequency, whereas for black holes of mass M, the late time frequency - from non-axisymmetric quadrupole mass motion about their Inner Most Stable Circular Orbit (ISCO,

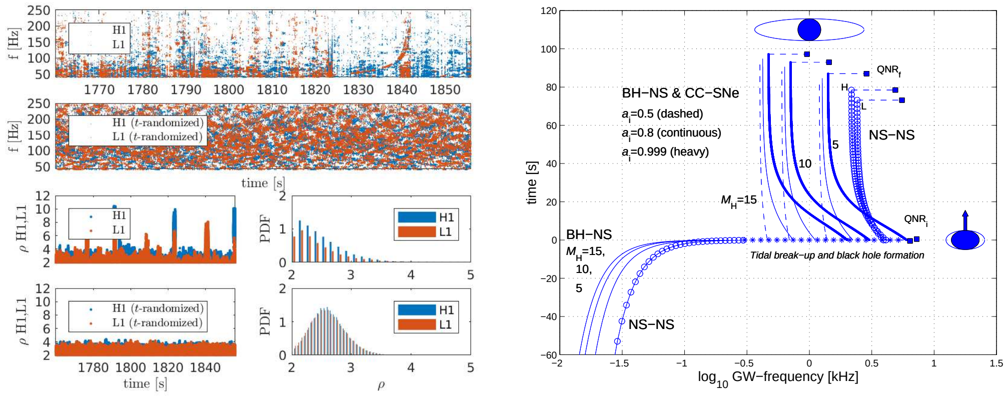

Fig. 2. (Left panels.) The merger GW170817 produces an *ascending* chirp in gravitational waves, here shown as the output of butterfly filtering of the LIGO H1 and L1 detectors, including control following time randomization (maximal entropy data). The left-truncated skewed Gaussians of maxima of butterfly output are markedly different for the original data and control. (Right panel.) Rotating black holes surrounded by a high density disk are a common outcome post-merger - of neutron stars with another neutron star or companion black hole - and core-collapse of massive stars. Black holes thus formed may spin rapidly, in which case they may loose angular momentum to high density matter at the Inner Most Stable Circular Orbit (ISCO) leading to catalytic conversion of spin energy to gravitational radiation (van Putten & Levinson 2003). In this process, the outcome is a *descending* chirp in gravitational waves for the lifetime of rapid spin. For GW170817 type events, the asymptotic result is tightly constraint by the narrow distribution of neutron star masses and spin (Baiotti et al. 2008), here indicated by H and L for high- and low-mass neutron stars. Absent a remnant stellar envelope, such binary merger creates a naked inner engine, whose magnetic winds may produce an observable radio burst. (Reprinted from (van Putten 2009).)

Kerr 1963; Bardeen et al. 1972) - reaches a late time plateau (van Putten et al. 2011a) (Fig. 2)

$$f_{GW} = (600 - 700)\,\mathrm{Hz}\left(\frac{M}{10M_\odot}\right)^{-1} \tag{1}$$

at a stationary point when the angular velocities of the black hole and matter at the ISCO are equal. In (1), the frequency uncertainty reflects variations in initial spin. For GW170817 like events with $M \simeq 3M_\odot$, f_{GW} would gradually settle down to a late time frequency of about 2000 Hz. This illustrates the need for high frequency multi-messenger probes to unambiguously identify GRB central engines. Establishing rotating black holes as central engines to GRBs and energetic core-collapse supernovae would give a first probe of relativistic frame dragging interactions with high density matter. Such measurement of gravitational interactions with matter is a limit of *strong* gravitation, representative for the theory of general relativity.

Extreme transient events such as GW170817 (Abbott et al. 2017a) and GRBs also have the potential to probe cosmological evolution (Amati 2012; Amati & Della Valle 2013, 2016) completely independent of the use of Type Ia supernovae and Cepheids. Already, GW170817 and its accompanying GRB170817A give an interesting estimate of the Hubble parameter H_0 (Guidorzi et al. 2017), completely independent of existing H_0 estimates. In general, cosmological evolution represents *weak* gravitational interactions about the de Sitter scale of acceleration

$$a_{dS} = cH, \tag{2}$$

set by the Hubble parameter $H = H(z)$ as a function of redshift z and velocity of light c.

Conceivably, weak gravitation takes us away from the geometric optics limit described by classical general relativity. In particular, evanescent dark energy and dark matter is expected from super-horizon scale fluctuations leaking in through the cosmological horizon (van Putten 2017c) (Fig. 3). According to the deceleration parameter

$$q(z) = -1 + (1+z)H^{-1}(z)H'(z), \quad (3)$$

the de Sitter limit ($q = -1, H'(z) = 0$) is hereby a *turning point* ($H'(z) = 0$) in cosmological evolution, showing a cosmological vacuum beyond the classical limit envisioned in general relativity.

The proposed *Transient High Energy Sky and Early Universe Surveyor* (THESEUS) mission (Amati et al. 2018) is designed to detect high-resolution light curves from GRBs over a broad range of redshift, which is ideally suited to pursue the above science in *strong and weak gravitational interactions* in central engines and, respectively, cosmological evolution.

For deep searches in broadband light curves of gamma-rays and gravitational radiation, we recently developed a new pipeline of butterfly filtering (§2), accelerated by *graphics processor units* (GPUs). §3 presents the need for accurate probes of $H(z)$ and $q(z)$ over an extended range of redshift z. We summarise these science objectives in §4.

2. Deep searches by butterfly filtering

2.1. Butterfly filtering

In powering extreme transient events - SGRBEEs, LGRBs and core-collapse supernovae - central engines exhaust their reservoir in angular momentum (for an early discussion in the context of core-collapse supernovae, see Bisnovatyi-Kogan 1970) over tens of seconds. Their output in electromagnetic and gravitational radiation will be unsteady and broadband with secular evolution in frequency, modulated by non-axisymmetric accretion flows (Fig. 4). For this reason, deep searches for their energetic output should be focused on frequencies that gradually vary in time, i.e., long duration ascending or descending chirps as opposed to constant frequencies. This may be approached by butterfly filtering, that essentially side-steps ordinary Fourier analysis (van Putten et al. 2014a; van Putten 2016). The resulting *chirp-based* spectrograms may reveal trajectories of frequency $f(t)$ with finite slope $df(t)/dt$, deteced by matched filtering using a large bank of templates, that are superpositions of ascending and descending chirps of intermediate duration, e.g., on the order of 1 s - an educated guess of potential phase-coherence on intermediate time scales.

Fig. 1 shows a demonstration in the identification of a broadband Kolmogorov spectrum in light curves of long GRBs at an on-average 1.26 photon per 0.5 ms bin from the *BeppoSAX* catalogue, using a bank of 8.64 million templates (van Putten et al. 2014a).

2.2. GPU acceleration

Fig. 2 shows an application to the gravitational strain data of the LIGO H1 and L1 output during GW170817, using a similar bank of 4 million templates. The ascending chirp of the binary neutron star merger identified should be compared with our control, produced by the same analysis following time-randomisation of the H1 and L1 data. (Time-randomisation produces data with maximal entropy, keeping histograms the same.)

Fig. 2 is computed by heterogeneous computing accelerated by high-end GPUs (van Putten 2017b), exploiting their high-performance processing of the Fast Fourier Transform (FFT, Fig. 5) and by circumventing bandwidth limitations of the *Peripheral Component Interface* (PCI) between GPU and the Central Processing Unit (CPU) using Parseval's Theorem. In this algorithm, only tails of butterfly output ρ exceeding $\kappa\sigma$, where κ parameterises the depth of the search ($\kappa > 1$), are communicated to the CPU. Under the *Open Compute Language* (OpenCL), this algorithm realises over one million correlations per second on a platform with 12 *Advanced Micro Devices* (AMD) Fiji chips with *High Bandwidth Memory 2* (HBM2) at an overall efficiency about 65%, normalized to clFFT GPU-performance. It enables a complete analysis of LIGO S6 by butterfly filtering against a

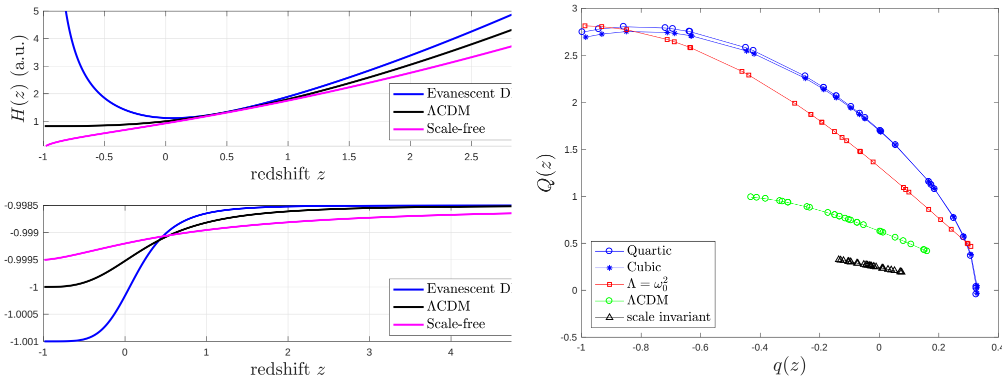

Fig. 3. (Left panel.) Evolution of the Hubble parameter $H(z)$ as a function of redshift according to evanescent dark energy, ΛCDM and a scale-free cosmology. (Right panel.) Confrontation of the three scenarios with heterogeneous $H(z)$ data over $0 < z < 1$ by nonlinear model regression, showing agreement of evanescent dark energy but not ΛCDM with model-independent fits by cubic and quartic polynomials. This result indicates that the de Sitter state ($q = -1, H'(z) = 0$) is a turning point, rather than an asymptotically stable state in ΛCDM. Similar analysis may be pursued by a large sample of GRBs covering an extended range of redshift. (Extended from (van Putten 2017c).)

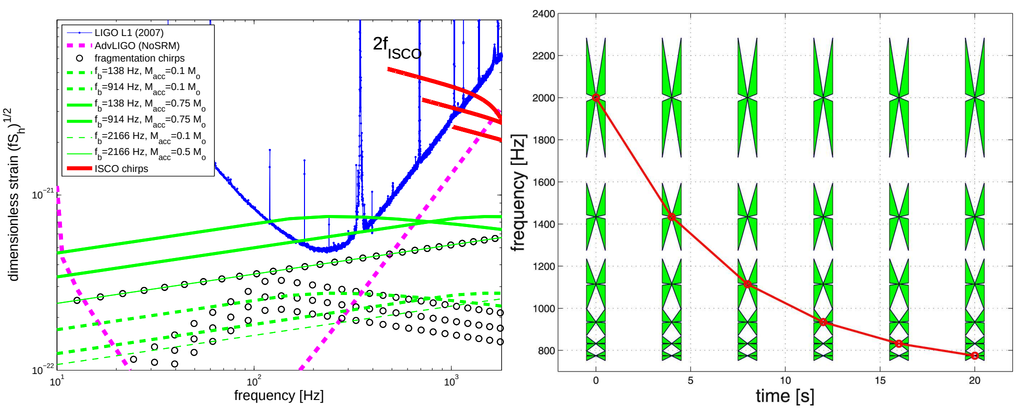

Fig. 4. (Left panel.) Characteristic strain $h_{char}(f)$ of quadrupole gravitational radiation from accretion flows around rotating black holes formed in core-collapse of massive stars at $D = 100$ Mpc. The vertical distance to the dimensionless strain detector noise $h_n = \sqrt{fS_h}$ represents the maximal attainable S/N ratio obtainable by filtering. Model curves shown are broadband emission from non-axisymmetric accretion flows (green), fragmentation chirps of (Piro & Pfahl 2007) (circles, $\sigma_f = 0.1$, $f_e = 120$ Hz) and ISCO waves induced by feedback from a central black hole (red). The curves shown refer to a black hole mass $M = 10M_\odot$ (black), $M = 7, 10$ and $15M_\odot$ (green, red). (Right panel.) Butterfly filtering is a bandpass filter of trajectories with finite slope $0 < \delta \leq df(t)/dt$ in frequency $f(t)$, suppresses signals with essentially constant frequencies, by matched filtering against a bank of a large number of templates of intermediate duration covering a broad bandwidth in frequency. (Reprinted from (Levinson et al. 2015; van Putten 2016).)

bank of up to 8 million templates within a one-year compute time (Fig. 6, comprising about 10^{20} floating point operations).

3. Probing the cosmological vacuum

High resolution measurements of the Hubble parameter $H(z)$ and the associated deceleration parameter (3) offer a detailed probe of the cosmological distributions of dark energy (Riess et al. 1998; Perlmutter et al. 1999). Late time evolution is particularly sensitive to the nature of dark energy (Fig. 3). While evolution in ΛCDM - with a static dark energy - is relatively stiff ($H'(0) \simeq 0.5H_0 > 0$), evolution is relatively fast with evanescent dark energy derived from super-horizon scale fluctuations ($H'(0) \simeq 0$). While the de Sitter state of cosmology is *assumed* to be the stable endpoint of cosmological evolution in ΛCDM, it is a turning point in evolution by (van Putten 2015, 2017c)

$$\Lambda = \omega_0^2 \quad (4)$$

from *evanescent fluctuations* (off-shell) at frequencies below the fundamental frequency

$$\omega_0 = \sqrt{1-q}H \quad (5)$$

of the cosmological horizon as an apparent horizon surface (Penrose 1965; Brewin 1988; York 1989; Wald & Iyer 1991; Cook & Abrahams 1992; Cook 2000; Thornburg 2007). With finite surface gravity away from the radiation dominated regime (Kodama 1980; Hayward 1998; Hayward et al. 1999; Bak & Rey 2000; Cai & Kim 2005), it gives rise to a stress energy tensor of the cosmological vacuum with nonzero trace, that is, a cosmological distriubution of evanescent dark energy and dark matter (van Putten 2018).

The qQ-diagram ($Q(z) = dq(z)/dz$), Fig. 3) shows a confrontation of these model alternatives $H(z) = \sqrt{1+\omega_m(6z+12z^2+12z^3+6z^4+(6/5)z^5)}/(1+z)$ and, respectively, $H(z) = \sqrt{1-\omega_m+\omega_m(1+z)^3}$, where ω_m denotes the cosmological density of matter (baryonic and cold) today, with tabulated data on $H(z)$ over an extended range of redshift of Farooq et al. (2017). Included is further a confrontation of recently proposed scale-free cosmologies (Maeder 2017; Jesus 2017). Agreement is found for evanescent dark energy with model-independent fits by cubic and quartic polynomials using nonlinear model regression. The latter rule out ΛCDM at a level of confidence of 2.7σ (van Putten 2017c). The resulting expectation for the Hubble parameter $H_0 = H(0)$ is

$$H_0 = 74.9 \pm 2.6 \mathrm{km\,s^{-1}Mpc^{-1}}, \quad (6)$$

consistent with Riess et al. (2016); Anderson & Riess (2017) and H_0 from GW170817 (Guidorzi et al. 2017).

In Fig. 3, *gap* in $Q_0 = Q(0)$, i.e., $Q_0 > 2.5$ for (4) and $Q_0 \lesssim 1$ for ΛCDM, represents a reformulation of the H_0 tension problem (Freedman 2017). Since this gap is of order unity, we expect that future samples of GW170817 type events and cosmological samples of GRBs from THESEUS over a broad range in redshifts will resolve this to better than the present 2.7σ (van Putten 2017c).

4. Conclusions

High frequency multi-messenger probes of light curves of GRBs will be instrumental in identifying their central engine, pertinent to resolving their physical origin and improving their potential as probes of cosmological evolution. Already, electromagnetic light curves increasingly point to black hole central engines rather than magnetars, at least for the soft extended emission common to SGRBEEs and normal LGRBs. Rigorous confirmation is expected from simultaneous detection of descending chirps in gravitational radiation, that may be identified in GW170817 like events in the near future or by detection of central engines to energetic core-collapse supernovae. THESEUS' design promises a significant advance to these science objectives, possibly in combination with an extended sample of GW170817 type events by LIGO-Virgo and KAGRA (Akutsu et al. 2018), in seeking answers to the questions: *What happened post-merger in GW170817?* Was the central engine to GRB170817A a magnetar or black hole? *What is the nature of the cosmological vacuum?* Is dark energy evanescent or constant, i.e., is the de Sitter state a turning point or an endpoint in cosmological evolution?

Acknowledgements. The author gratefully acknowledges stimulated discussions with L. Amati, F. Frontera, M. Della Valle, A.J. Weinstein

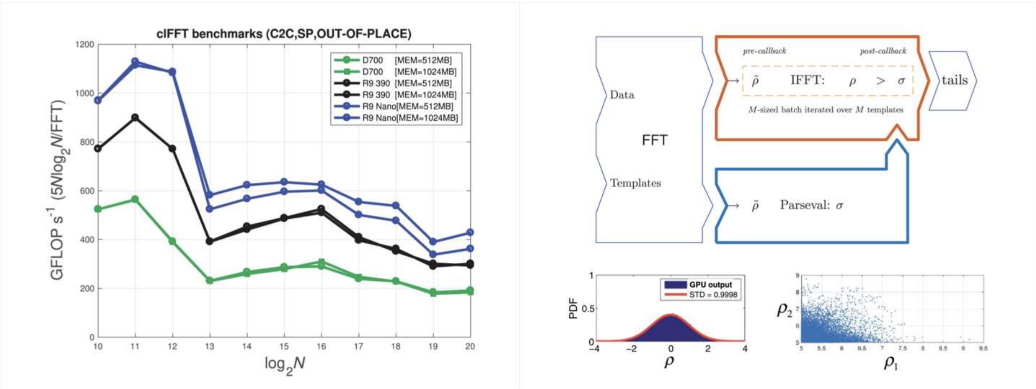

Fig. 5. GPU benchmark results on clFFT$_N$ under OpenCL for complex-to-complex (C2C) single precision (SP) with out-of-place allocation in Global Memory for various high-end GPUs of Advanced Micro Devices (AMD). For data-segments of 16 seconds ($N = 2^{16}$ at a sampling rate of 4096 s^{-1}), the R9 Nano with High Bandwidth Memory 2 (HBM2) enables about 100,000 transforms per second. Efficient GPU-acceleration obtains by circumventing limitations of the PCI by communicating only tails $\rho > \kappa\sigma$ back to the CPU from Global Memory in the GPU, where $\kappa > 1$ defines the search depth and σ is the standard deviation of the matched filtered output ρ, computed in a predictor step by Parseval's Theorem (also off-loaded to the GPU). (Reprinted from (van Putten 2017b).)

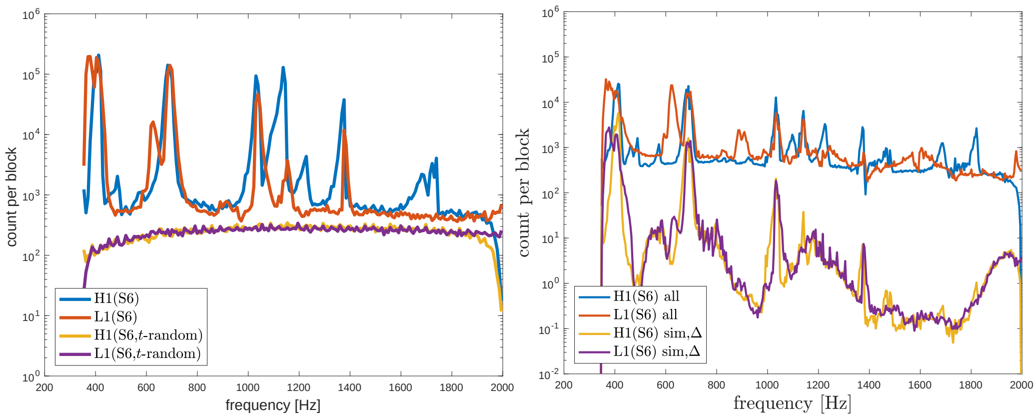

Fig. 6. (Left) Pseudo-spectra of simultaneous $\rho > \kappa\sigma$ in H1 (red) and L1 (blue), averaged over four blocks of S6 H1∧ L1, using a bank of 8M templates, along with control using maximal entropy (time-randomized) data. (Right) Pseudo-spectra as an average over all 288 blocks of S6 H1∧L1, using a bank of 0.5M templates, of H1 and L1 by independent counts and by simultaneous counts with frequency pairs within Δf = 50 Hz. (Reprinted from (van Putten 2017b).)

and J.B. Kanner and support from NRF of Korea under 2015R1D1A1A01059793 and 2016R1A5A1013277. LIGO S6 and O2 data are from LOSC provided by LIGO and the LSC. LIGO is funded by the U.S. NSF. Additional support is from MEXT, JSPS Leading-edge Research Infrastructure Program, JSPS Grant-in-Aid for Specially Promoted Research 26000005, MEXT Grant-in-Aid for Scientific Research on Innovative Areas 24103005, JSPS Core-to-Core Program, Advanced Research Networks jointly with the ICRRR, Tokyo.

References

Abbott, B. P., Abbott, R., Abbott, T. D., et al. 2017, Phys. Rev. Lett., 119, 161101

Akutsu, T., et al. 2018, Progress of Theoretical and Experimental Physics, 013F01
Amati, L, et al. 2002, A&A, 390, 89
Amati, L. 2012, Int. J. of Modern Physics: Conf. Ser., 12, 19
Amati, L., & Della Valle, M. 2013, Int. J. of Modern Physics D, 22, 1330028
Amati, L., & Della Valle, M. 2016, A&A Tr., 29, 193
Amati, L., et al. 2018, Adv. Space Res., 62, 191
Anderson, R. I., & Riess, A. G. 2017, arXiv:1712.01065v1
Baiotti, L., Giacomazzo, B., & Rezzolla, L. 2008, Phys. Rev. D, 78, 084033
Bak, D., & Rey, S.-J. 2000, Class. Quant. Grav., 17, L83
Bardeen, J. M., Press, W. H., & Teukolsky, S. A. 1972, Phys. Rev. D, 178, 347
Bisnovatyi-Kogan, G. S. 1970, Astron. Zh., 47, 813
Brewin, L. 1988, Phys. Rev. D, 38, 3020
Cai, R.-G., & Kim, S. P. 2005, J. of High Energy Phys., 2, 50
Carter, B. 1968, Phys. Rev., 174, 1559
Cook, G. B., & Abrahams, A. M. 1992, Phys. Rev. D, 46, 702
Cook, G. B. 2000, Living Reviews Relativity, 3, 5
Cutler, C., & Thorne, K. S. 2002, in Proceedings of the 16th International Conference on General Relativity & Gravitation, ed. N. T. Bishop and S. D. Maharaj (World Scientific Publ., Singapore), 72
Eichler, D. & Levinson, A. 2000, ApJ, 529, 146
Farooq, O., Madiyar, F. R., Crandall, S., & Ratra, B. 2017, ApJ, 835, 26
Freedman, W. L. 2017, Nature Astronomy, 1, 0121
Guidorzi, C., et al. 2017, ApJ, 851, L36
Hayward, S. A. 1998, Class. Quant. Grav., 15, 3147
Hayward, S. A., Mukohyama, S., & Ashworth, M. C. 1999, Phys. Lett. A, 256, 347
Jesus, J. F. 2017, arXiv:1712.00697
Kerr, R. P. 1963, Phys. Rev. Lett., 11, 237
Kodama, H. 1980, Progr. Theor. Phys., 63, 1217
Levinson, A., van Putten, M. H. P. M., & Pick, G. 2015, ApJ, 812, 124
Maeder, A. 2017, ApJ, 849, 194
Metzger, D. B., et al. 2011, MNRAS, 413, 2031
Nakar, E. 2007, Phys. Rep., 442, 166
Penrose, R. 1965, Phys. Rev. Lett., 14, 57
Perlmutter, S., et al. 1999, ApJ, 517, 565
Piran, T. 2004, Reviews of Modern Physics, 76, 1143
Piro, A. L., & Pfahl, E. 2007, ApJ, 658, 1173
Riess, A., et al. 1998, ApJ, 116, 1009
Riess, A. G., et al. 2016, ApJ, 826, 56
Sari, R., & Piran, T. 1997, ApJ, 485, 270
Sari, R., Piran, T., & Narayan, R. 1998, ApJ, L17
Thornburg, J. 2007, Living Reviews in Relativity, 10, 3
van Putten, M. H. P. M., & Levinson, A. 2003, ApJ, 584, 937
van Putten, M. H. P. M. 2009, MNRAS, 396, L81
van Putten, M. H. P. M., et al. 2011a, Phys. Rev. D 83, 044046
van Putten, M. H. P. M. 2012a, Prog. Theor. Phys., 127, 331
van Putten, M. H. P. M., Guidorzi, C., & Frontera, P. 2014a, ApJ, 786, 146
van Putten, M. H. P. M., et al. 2014, MNRAS, 444, L58
van Putten, M. H. P. M. 2015, MNRAS, 450, L48
van Putten, M. H. P. M. 2016, ApJ, 819, 169
van Putten, M. H. P. M., & Della Valle, M. 2017, MNRAS, 464, 3219
van Putten, M. H. P. M. 2017, Progress of Theoretical and Experimental Physics, 93F01
van Putten, M. H. P. M. 2017, ApJ, 848, 28
van Putten, M. H. P. M. 2018, under review
Wald, R. M., & Iyer, V. 1991, Phys. Rev. D, 44, R3719
Woosley, S. L. 1993, ApJ, 405, 273
Woosley, S. E., & Bloom, J. S. 2006, ARA&A, 44, 507
Woosley, S. E. 2010, ApJ, 719, L204
York, J. W. 1989, in Frontiers in Numerical Relativity, ed. C. R. Evans, L. S. Finn & D. W. Hobill (Cambridge University Press), 89

Zigao, D., Frédéric, D., & Mészáros, P. 2017, Space Sci. Rev., 212, 409

Zhang, B., Lü, H.-J., & Liang, E.-W. 2016, Space Sci. Rev., 202, 3